A comparative study between CMGs and RWs in small satellite attitude control

Qiang Shen
Temasek Laboratories
National University of Singapore
Singapore, Singapore 117411
Email: tslshen@nus.edu.sg

Cher Hiang Goh, Chengfei Yue, Dan Feng, and Wei Han Ee
Department of Electrical and Computer Engineer
National University of Singapore
Singapore, Singapore 117582
Email: elegch@nus.edu.sg; e0011355@u.nus.edu; {elefeng, eleewhe}@nus.edu.sg

***Abstract*—This paper investigates the operational unique features in using control moment gyroscopes (CMGs) and reaction wheels (RWs) for small satellite attitude control applications. Singapore had designed and launched their 1st micro-satellite (X-Sat) in April 2011 and had recently launched another 6 satellites in December 2015. Besides the nano-satellites, the various micro-/small-satellites employed reaction wheels (RWs) for attitude control to accomplish its mission operations. To look into enhancing operational values of future satellite missions, we considered a high agility spacecraft attitude control as a key technology enable. Here, we examined the application specifics of CMGs and RWs for spacecraft attitude control application by working through the different working principle of these actuators on changing the stored angular momentum. We analysed the different application constraints and attitude maneuver performance that can be achieved by such actuators (CMGs/RWs). Advantages and limitations of each actuator are analyzed at philosophical level, and quantitative assessments are conducted through numerical simulations on a typical microsatellite we planned for the next/future satellite mission. Specifically, the control performances such as maneuver agility, torque generation, and design complexity of steering law, have been examined subject to identical pointing requirements and operating condition as a reference. The contributions of this paper will benefit mission designer a sound assessment on the actuator for use that is better suited to the particular mission.**

I. Introduction

Interest in small satellites for earth observation, communication, navigation and science mission has grown over years due to a number of factors: shorter design periods, lower mass to reach orbit, and less costs. Singapore had designed and launched their 1st micro-satellite (X-Sat) in April 2011 and had recently launched another 6 small satellites in December 2015. For next generation of Singapore's satellite, it is required to have a smaller size while achieving rapid rotational agility and high pointing accuracy, which gives rise to challenges to attitude determination and control systems (ADCS). Control moment gyros (CMGs) and reaction wheels (RWs) are two commonly used actuators in ADCS for small satellite due to their small volume and light weight.

CMGs posses the typical torque amplification characteristics that significantly enhance the controllability and agility, and attract great attentions for small satellite missions with rapid slew rates and high pointing accuracy requirements. During the past two decades, CMGs-based spacecraft attitude control systems have been studied extensively in literature, in which most of the existing works focus on developing CMG steering law to handle singularity. At singular configurations, CMGs are unable to exactly produce the required torque in certain directions. In order to deal with this CMGs singularity problem, several papers present various solutions such as singular escape method [1], [2] and singular avoidance method [3]–[5]. However, most of the solutions are fairly complex so that they cannot be implemented in onboard computer. In space applications, CMGs have been successfully employed for a variety of large spacecraft, such as the Skylab, the MIR space station, and the International Space Station. For small satellite, using CMGs as actuators is still in the process of laboratory test.

RW doesn't have singularity problem and typically have a much simple steering logic than that of CMGs. Since RWs have a simple structure and operation mechanism, many available commercial RWs exist in the market and they have been widely used in space missions. Drawbacks to the reaction wheels include a relatively small effective torque being produced on the spacecraft and the possibility of reaction wheel saturation. In addition, RWs typically require more energy than CMGs to produce a given torque onto a spacecraft. In literature, research on RWs mainly concentrates on torque distribution [6], [7], fault-tolerant capability [8]–[10], and saturation compensation [11], [12].

This paper conducts a comparative study between CMGs and RWs from attitude control perspective. Attitude dynamics of a rigid spacecraft equipped with 4 SGCMGs or 4 RWs as actuators is modeled separately. Based on these models, steering laws for CMGs and RWs are given to achieve the commanded control torques generated by attitude controller. Through simulations of attitude control system of a small satellite, the control performances such as maneuver agility, pointing accuracy, power consumption, and design complexity under CMGs and RWs are analyzed and compared. The results from the analysis give the mission designer an assessment on the actuator that is better suited for the particular mission.

II. Dynamic Models

A simple block diagram representation of a CMGs/RWs-based attitude control system is illustrated in Figure 1. The

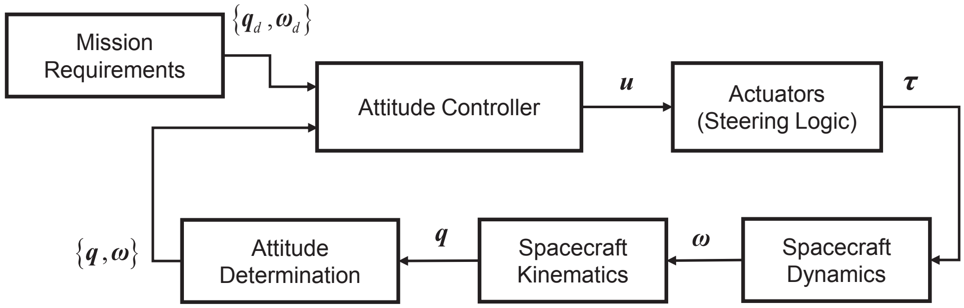

Fig. 1. A CMGs/RWs-based attitude control system.

nature of CMGs and RWs, their torque and momentum capabilities, as well as their precision and speed of response, determines their usefulness for the range of missions that spacecraft are intended to achieve. When CMGs or RWs are used as actuator for attitude control, the total angular momentum is made up of the spacecraft main body angular momentum and the actuator angular momentum, which can be expressed in the body fixed frame as follows

$$\boldsymbol{H} = \boldsymbol{J}\boldsymbol{\omega} + \boldsymbol{A}\boldsymbol{h}, \tag{1}$$

where $\boldsymbol{J}$ is the inertia tensor, $\boldsymbol{\omega}$ is the angular velocity vector of the spacecraft, $\boldsymbol{A}$ is the transformation matrix from the wheel frame to spacecraft body frame, $\boldsymbol{h}$ is the angular momentum produced by CMGs/RWs cluster. The equations of motion are derived by taking the time derivative of the total angular momentum of the system. The time derivative of $\boldsymbol{H}$ in the body frame is

$$\boldsymbol{J}\dot{\boldsymbol{\omega}} + \boldsymbol{\omega}^{\times}\boldsymbol{J}\boldsymbol{\omega} = \boldsymbol{\tau} + \boldsymbol{T}_{ext} \tag{2}$$

$$\boldsymbol{\tau} = -(\dot{\boldsymbol{A}}\boldsymbol{h} + \boldsymbol{A}\dot{\boldsymbol{h}}) - \boldsymbol{\omega}^{\times}\boldsymbol{A}\boldsymbol{h} \tag{3}$$

where $\boldsymbol{T}_{ext}$ is external torque such as external disturbances, $\boldsymbol{\tau}$ is the internal control torque generated by CMGs/RWs. The notation $\boldsymbol{a}^{\times}$ for a vector $\boldsymbol{a} = [a_1 \quad a_2 \quad a_3]^T$ is used to represent the skew-symmetric matrix

$$\boldsymbol{a}^{\times} = \begin{bmatrix} 0 & -a_3 & a_2 \\ a_3 & 0 & -a_1 \\ -a_2 & a_1 & 0 \end{bmatrix}. \tag{4}$$

Since CMGs and RWs operate through different working principle on changing the stored angular momentum, the equations of attitude dynamics for spacecraft equipped with CMGs and RWs are different.

A. Attitude Dynamics with CMGs

A CMG contains a spinning rotor with large angular momentum, but whose angular momentum vector (direction) can be changed with respect to the spacecraft by gimballing the spinning rotor. A typical single gimbal control moment gyro (SGCMG) is shown in Figure 2, in which the rotor spins at a constant speed. The angular moment vector $\boldsymbol{h}_i$ points along the spindle axis, the gimbal axis is always orthogonal to the spin axis and is denoted by $\boldsymbol{g}_i$, the output torque axis $\boldsymbol{t}_i = \boldsymbol{g}_i \times \boldsymbol{h}_i$ is orthogonal to both $\boldsymbol{g}_i$ and $\boldsymbol{h}_i$. The subscript i denotes the ith SGCMG. Vectors $\boldsymbol{g}_i$, $\boldsymbol{h}_i$ and $\boldsymbol{t}_i$ form the right hand orthogonal CMG frame and they are the unit vector in their direction. The CMG is a torque amplification device as a small gimbal torque input produces a large control torque output on the spacecraft. Because CMGs are capable of generating large control torques and angular momentum, they are often favored for precision pointing and tracking control of agile spacecraft in low Earth orbit.

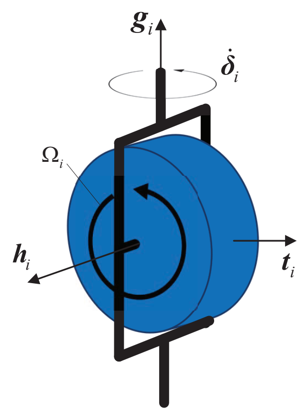

Fig. 2. Single gimbal control moment gyro.

For three-axis attitude control of spacecraft, four SGCMGs in a pyramid configuration are usually selected, and the skew angle is chosen as $\beta = 54.73$ deg so that the momentum envelope is nearly spherical. Assuming that the angular momentum vector of each SGCMG has the same magnitude h_0, the total angular momentum is expressed as

$$\begin{aligned} \boldsymbol{h}_{CMG} &= \boldsymbol{h}_1 + \boldsymbol{h}_2 + \boldsymbol{h}_3 + \boldsymbol{h}_4 \\ &= \boldsymbol{A}[\ h_0 \quad h_0 \quad h_0 \quad h_0\ ]^T, \end{aligned} \tag{5}$$

where $\boldsymbol{A}$ is the transformation matrix from the gimbal frame to spacecraft body frame given by

$$\boldsymbol{A} = \begin{bmatrix} -c\beta\sin\delta_1 & -\cos\delta_2 & c\beta\sin\delta_3 & \cos\delta_4 \\ \cos\delta_1 & -c\beta\sin\delta_2 & -\cos\delta_3 & c\beta\sin\delta_4 \\ s\beta\sin\delta_1 & s\beta\sin\delta_2 & s\beta\sin\delta_3 & s\beta\sin\delta_4 \end{bmatrix}$$

with $c\beta \equiv \cos\beta$, $s\beta \equiv \sin\beta$. The transformation matrix $\boldsymbol{A}$ of SGCMG is in general a function of CMG gimbal angle $\boldsymbol{\delta}$.

Specifically, for SGCMGs, since each flywheel has a constant spinning speed, it is clear that $\boldsymbol{A}\dot{\boldsymbol{h}} = 0$. Moreover, the time derivative of the transformation $\boldsymbol{A}$ is obtained as

$$\dot{\boldsymbol{A}} = \overline{\boldsymbol{A}}\dot{\boldsymbol{\delta}}, \tag{6}$$

where $\overline{\boldsymbol{A}}$ is the Jacobian matrix defined as

$$\overline{\boldsymbol{A}} = \begin{bmatrix} -c\beta\cos\delta_1 & \sin\delta_2 & c\beta\cos\delta_3 & -\sin\delta_4 \\ -\sin\delta_1 & -c\beta\cos\delta_2 & \sin\delta_3 & c\beta\cos\delta_4 \\ s\beta\cos\delta_1 & s\beta\cos\delta_2 & s\beta\cos\delta_3 & s\beta\cos\delta_4 \end{bmatrix}.$$

Therefore, the internal control torque $\boldsymbol{\tau}$ generated by SGCMGs in (3) is reduced to

$$\boldsymbol{\tau} = -h_0\overline{\boldsymbol{A}}\dot{\boldsymbol{\delta}} - \boldsymbol{\omega}^{\times}\boldsymbol{A}\boldsymbol{h}_{CMG}. \tag{7}$$

B. Attitude Dynamics with RWs

A RW is a type of flywheel with an electric motor attached. Changing the rotation speed of flywheel causes the spacecraft to begin to counter-rotate proportionately through conservation of angular momentum. A typical RW is shown in Figure 3. The output torque is given as $\boldsymbol{t}_i = \dot{\boldsymbol{h}}_i$. Comparing to CMGs, the RWs have a simple mechanical structure, but they have much smaller control torque capability.

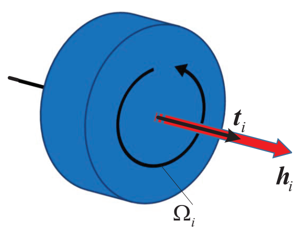

Fig. 3. Reaction wheel.

Similar to CMGs, four RWs are commonly used for three-axis attitude control, which provides a redundant set of RW for fault-tolerant consideration. The total angular momentum generated by RWs is

$$\begin{aligned} \boldsymbol{h}_{RW} &= \boldsymbol{h}_1 + \boldsymbol{h}_2 + \boldsymbol{h}_3 + \boldsymbol{h}_4 \\ &= J_W\boldsymbol{A}\boldsymbol{\Omega}, \end{aligned} \tag{8}$$

where J_W is moment inertia of RW, and $\boldsymbol{\Omega} = [\Omega_1 \quad \Omega_2 \quad \Omega_3 \quad \Omega_4]^T$.

Once RWs array is determined, the transformation matrix from the wheel frame to spacecraft body frame is fixed as well. That is to say, the matrix $\boldsymbol{A}$ is a constant matrix that only depends on the assemble direction angles. As a result, it is obtained that $\dot{\boldsymbol{A}} = 0$ in normal attitude maneuvers. The internal control torque $\boldsymbol{\tau}$ generated by RWs in (3) is reduced to

$$\boldsymbol{\tau} = -J_W\boldsymbol{A}\dot{\boldsymbol{\Omega}} - \boldsymbol{\omega}^{\times}\boldsymbol{A}\boldsymbol{h}_{RW}. \tag{9}$$

III. Steering Logics

The utilization of CMGs/RWs necessitates the development of CMGs/RWs steering logic, which drive the CMGs/RWs to generate the commanded spacecraft control torques from attitude controller. That is, the steering logic transfers the control torques from system level to actuator level. Assuming that the commanded control torque $\boldsymbol{u}$ is computed by a proper attitude controller for achieving the desired three-axis attitude maneuver, then the steering law should be designed such CMGs/RWs realize the commanded control torque, i.e., $\boldsymbol{\tau} = \boldsymbol{u}$. One of the major issues in using CMGs for spacecraft attitude control is the CMG geometric singularity problem in which no control torque is generated for the commanded control torque along a particular direction. However, RWs do not have such a singularity problem.

A. Steering Logic for CMGs

Based on the equation in (7), the following relation can be obtained

$$\boldsymbol{\tau} = \boldsymbol{u} = -h_0\overline{\boldsymbol{A}}\dot{\boldsymbol{\delta}} - \boldsymbol{\omega}^{\times}\boldsymbol{A}\boldsymbol{h}_{CMG}. \tag{10}$$

It means that the CMG steering logic should determine the gimbal rate $\dot{\boldsymbol{\delta}}$ that can generate the commanded control torque $\boldsymbol{u}$. The basic solution of $\dot{\boldsymbol{\delta}}$ for above equation is referred to as the peseudoinverse steering logic, which is given by

$$\dot{\boldsymbol{\delta}} = -\frac{1}{h_0}\overline{\boldsymbol{A}}^{\dagger}(\boldsymbol{u} + \boldsymbol{\omega}^{\times}\boldsymbol{A}\boldsymbol{h}_{CMG}), \tag{11}$$

where the peseudoinverse is defined as $\overline{\boldsymbol{A}}^{\dagger} = \overline{\boldsymbol{A}}^T(\overline{\boldsymbol{A}}\,\overline{\boldsymbol{A}}^T)^{-1}$. As mentioned earlier that the Jacobian matrix $\overline{\boldsymbol{A}}$ is a function of gimbal angle $\boldsymbol{\delta}$, the CMG steering logic may encounter singularity if rank$(\overline{\boldsymbol{A}}) < 3$ for certain sets of gimbal angles.

Several approaches for avoiding or escaping CMGs singular states have been proposed in literature. Here, one of the most commonly used method, the general singular robust (GSR) steering law [1], is employed to handle CMG singularity. According to GSR steering law, the gimbal rate that can generate the commanded torque is given by

$$\dot{\boldsymbol{\delta}} = -\frac{1}{h_0}\overline{\boldsymbol{A}}^{\sharp}\left(\boldsymbol{u} + \boldsymbol{\omega}^{\times}\boldsymbol{A}\boldsymbol{h}_{CMG}\right), \tag{12}$$

where $\overline{\boldsymbol{A}}^{\sharp} = \overline{\boldsymbol{A}}^T\left[\overline{\boldsymbol{A}}\,\overline{\boldsymbol{A}}^T + \alpha\boldsymbol{E}\right]^{-1}$, $\alpha = \alpha_0\exp\left(-\mu m^2\right)$, $m = \sqrt{\det\left(\overline{\boldsymbol{A}}\,\overline{\boldsymbol{A}}^T\right)}$ is the singularity measure. The matrix $\boldsymbol{E}$ is defined as

$$\boldsymbol{E} = \begin{bmatrix} 1 & \varepsilon_3 & \varepsilon_2 \\ \varepsilon_3 & 1 & \varepsilon_1 \\ \varepsilon_2 & \varepsilon_1 & 1 \end{bmatrix}, \quad \varepsilon_i = \varepsilon_0\sin(\varpi_i t + \phi_i) \tag{13}$$

where ε_i, ϖ_i and ϕ_i are properly selected.

B. Steering Logic for RWs

For RWs, according to equation (9), the following relation can be obtained

$$\boldsymbol{\tau} = \boldsymbol{u} = -J_W \boldsymbol{A}\dot{\boldsymbol{\Omega}} - \boldsymbol{\omega}^{\times} \boldsymbol{A}\boldsymbol{h}_{RW}. \tag{14}$$

It means that the RW steering logic should determine the wheel acceleration $\dot{\boldsymbol{\Omega}}$ that can generate the commanded control torque $\boldsymbol{u}$. Since the transformation matrix $\boldsymbol{A}$ is constant, the pseudoinverse of $\boldsymbol{A}$ always exists. Therefore, the pseudoinverse steering logic can be used for RWs directly and is given by

$$\dot{\boldsymbol{\Omega}} = -\frac{1}{J_W} \boldsymbol{A}^{\dagger} \left(\boldsymbol{u} + \boldsymbol{\omega}^{\times} \boldsymbol{A}\boldsymbol{h}_{RW} \right), \tag{15}$$

where $\boldsymbol{A}^{\dagger} = \boldsymbol{A}^T (\boldsymbol{A}\boldsymbol{A}^T)^{-1}$.

IV. Simulation Results

A. Simulation Specification

In this section, satellite attitude control with CMGs/RWs is studied through simulation. The Kent Ridge 1 (KR-1) satellite is considered as simulation model (see Figure 4). Table I contains the satellite parameters used for the simulations.

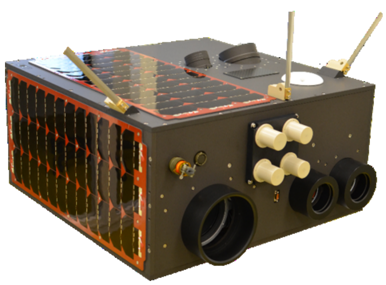

Fig. 4. Kent Ridge 1 satellite.

TABLE I
Simulation parameters

Parameter	value
Mass (kg)	79
Size (mm)	575×572×384
Moment of inertia (kg·m^2)	$\boldsymbol{J}_1 = 3.34$, $\boldsymbol{J}_2 = 5.29$, $\boldsymbol{J}_3 = 3.21$
Slew capacity (deg/s)	$\lvert\omega_1\rvert_{\max} = 8.8$, $\lvert\omega_2\rvert_{\max} = 5.5$, $\lvert\omega_3\rvert_{\max} = 9.1$
Initial attitude	$\boldsymbol{Q}(0) = [0 \quad 0 \quad 0 \quad 1]^T$
Initial rate (deg/s)	$\boldsymbol{\omega}(0) = [0 \quad 0 \quad 0]^T$

Four SGCMGs in a regular pyramid configuration is used in simulation. The specification of SGCMG is shown in Table II. The initial gimbal angles are selected as $\boldsymbol{\delta}(0) = [0 \quad 0 \quad 0 \quad 0]^T$ deg, which are far way from singular states. The parameters in GSR steering law described in equation (12) are selected as:

$$\alpha_0 = 0.01, \quad \mu = 10, \quad \phi_1 = 0, \quad \phi_2 = \frac{\pi}{2}, \quad \phi_3 = \pi,$$
$$\epsilon_i = 0.01 \sin(0.5\pi t + \phi_i), \quad i = 1, 2, 3. \tag{16}$$

TABLE II
SGCMGs parameters

Parameter	value
Skew angle (deg)	54.74
Maximum momentum (Nms)	$h_{\max} = 1$
Maximum output torque (Nm)	$\tau_{\max} = 1$
Maximum gimbal rate (deg/s)	$\dot{\delta}_{\max} = 30$

For comparison, KR-1 satellite with four RWs is also simulated. The configuration of four RWs is shown in Figure 5, in which the rotation axes of three RWs (such as RWs 1, 2, and 3) are orthogonal to the spacecrafts orthogonal shaft, and the fourth one is installed with the equiangular direction with the orthogonal-to-each other three axes. The specifications of the RWs are shown in Table III such so that they will have approximately the same size as in the case of CMGs.

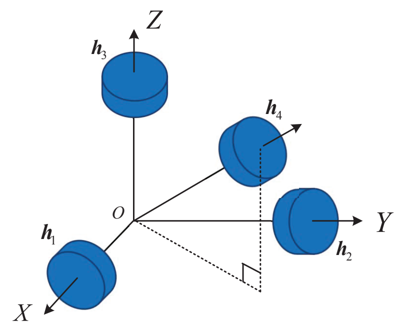

Fig. 5. Configuration of four reaction wheels.

TABLE III
RWs parameters

Parameter	value
Mass (kg)	1.7
Size (mm)	100×100×80
Maximum momentum (Nms)	$h_{\max} = 0.5$
Maximum output torque (mNm)	20

B. Attitude Controller Design

The KR-1 satellite is required to maneuver about an inertially fixed axis as fast as possible, but not exceeding the specified maximum slew rate about that eigenaxis. Meanwhile, assuming that the control torque input for each axis is constrained as

$$-U \leq u_i(t) \leq +U, \quad i = 1, 2, 3 \tag{17}$$

where U is the saturation limit of each control limit. The following cascaded saturation control logic provides such a rest-to-rest eigenaxis rotation under slew rate and control input constraints [13]:

$$\boldsymbol{u} = -\operatorname*{sat}_{U}\left\{\boldsymbol{J}\left(2k\operatorname*{sat}_{L_i}(\boldsymbol{q}_e) + c\boldsymbol{\omega}\right)\right\}, \tag{18}$$

where k and c are two gains, the saturation function is defined as

$$\operatorname*{sat}_{U}(u_i) = \begin{cases} U & u_i \geq U \\ u_i & |u_i| < U \\ -U & u_i \leq -U. \end{cases} \tag{19}$$

The saturation limits L_i is determined as

$$L_i = \frac{c}{2k}\min\left\{\sqrt{4a_i|\boldsymbol{q}_{e,i}|}, |\omega_i|_{max}\right\}, \tag{20}$$

where $a_i = U/J_{ii}$ is the maximum control acceleration about the ith control axis, and $|\omega_i|_{max}$ is the specified maximum angular rate about each axis. More details about this cascade-saturate quaternion feedback control law can be found in reference [13]. In simulations, the parameters in cascade-saturate attitude controller proposed in equation (18) are selected as $k = 17.22$ and $c = 7.55$.

C. Single-Axis Attitude Control Case

In the first case, the spacecraft are required to perform a single-axis attitude maneuver with 60 deg rotation in roll axis. The simulation results are shown in Figures 6 to 9. Figures 6a and 6b depict the attitude responses of KR-1 satellite controller by CMGs and RWs, respectively. It is clear that attitude of CMGs-controlled spacecraft is stabilized in 7.48 seconds, while RW-controlled satellite needs more than 40 seconds to achieve the same control accuracy. That is to say, the agility of CMGs-controlled satellite is about 5.4 times better than that of RWs-controlled satellite in single-axis large attitude maneuver. Similar results are also observed in angular velocity responses under two different actuators in Figures 7a and 7b. Output torques provided by CMGs and RWs are shown in Figures 8a and 8b, respectively. It is clear that CMGs generate a larger torque than that of RWs. Consequently, the slew rate of CMGs-based satellite is also larger than that of RWs-based satellite. Since the initial gimbal angles of CMGs are far away from the singular states, the singularity measure is not approaching to zero as shown in Figure 9a. Figure 9b shows the gimbal rate response, from which it is clear that each gimbal rate is constrained within its maximal value.

D. Three-Axis Attitude Control Case

In the second case, three-axis attitude maneuver is simulated, and rotations of 70 deg, -22.6 deg, and 30 deg in roll, pitch, and yaw axis are required, respectively. The simulation results are shown in Figures 10 to 13. Figures 10a and 10b show the attitude responses under CMGs and RWs when three-axis attitude maneuver is required. It is observed that attitude of CMG-controlled spacecraft is stabilized in 9.4 seconds, while RW-controlled satellite needs more than 42.5 seconds to achieve the same control accuracy. Based on the above observation, it is found that the agility of CMGs-controlled

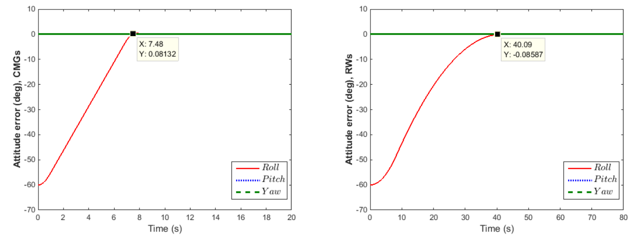

(a) Euler angle, CMG (b) Euler angle, RW

Fig. 6. Euler angle in single-axis attitude maneuver using CMGs and RWs.

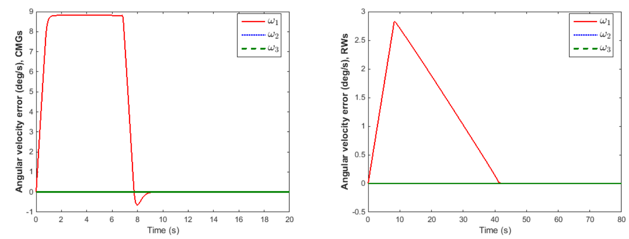

(a) Angular velocity, CMG (b) Angular velocity, RW

Fig. 7. Angular Velocity in single-axis attitude maneuver using CMGs and RWs.

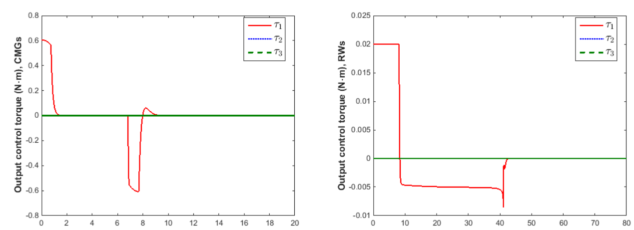

(a) Output torque, CMG (b) Output torque, RW

Fig. 8. CMGs and RWs output torques in single-axis attitude maneuver.

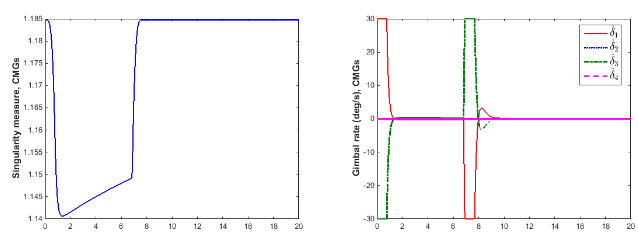

(a) CMG singularity measure (b) CMG gimbal rate

Fig. 9. Singularity measure and gimbal rate of CMGs in single-axis attitude control case.

satellite is about 4.5 times better than that of RWs-controlled satellite in three-axis large attitude maneuver. From Figures 11a and 11b, it is clear that the CMGs-controlled satellite has a larger slew rate than that of RWs-controlled satellite. Output torques provided by CMGs and RWs are shown in Figures 12a and 12b, respectively. It is shown that CMGs generate a larger torque than that of RWs. The singularity measure is always greater than zero as shown in Figure 13a, which means that no CMG singularity occurs during this maneuver. Figure 13b shows the gimbal rate response, from which it is clear that gimbal rate constraints are satisfied in the simulation.

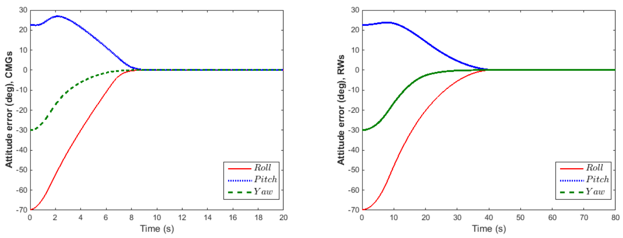

(a) Euler angle, CMG (b) Euler angle, RW

Fig. 10. Euler angle in three-axis attitude maneuver using CMGs and RWs.

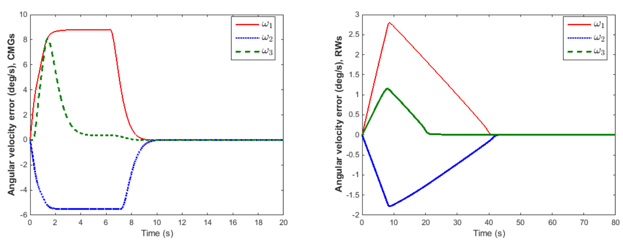

(a) Angular velocity, CMG (b) Angular velocity, RW

Fig. 11. Angular Velocity in single-axis attitude maneuver using CMGs and RWs.

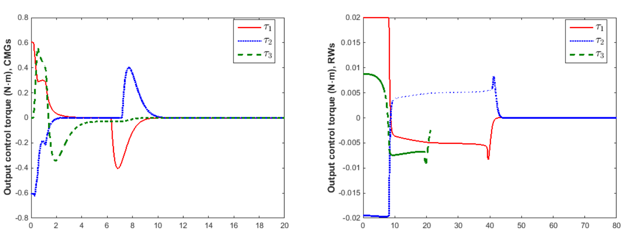

(a) Output torque, CMG (b) Output torque, RW

Fig. 12. CMGs and RWs output torques in three-axis attitude maneuver.

V. Conclusions

In this paper a comprehensive comparison between CMGs and RWs for spacecraft attitude control is conducted. Mathematic models of spacecraft equipping with CMGs/RWs are established. Simulation results show that CMGs-based satellite

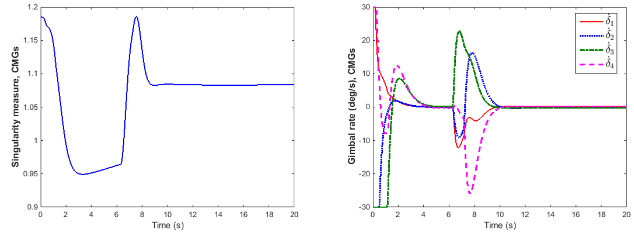

(a) CMG singularity measure (b) CMG gimbal rate

Fig. 13. Singularity measure and gimbal rate of CMGs in three-axis attitude control case.

achieves 4 to 5 times improvement in maneuver time of large-angle attitude control comparing with RWs-based satellite. However, RWs have a less structure complex and their steering logic can be designed easily in the comparison of CMGs.

References

[1] B. Wie, D. Bailey, and C. Heiberg, "Singularity robust steering logic for redundant single-gimbal control moment gyros," *Journal of Guidance, Control, and Dynamics*, vol. 24, no. 5, pp. 865–872, 2001.

[2] B. Wie, "Singularity analysis and visualization for single-gimbal control moment gyro systems," *Journal of Guidance, Control, and Dynamics*, vol. 27, no. 2, pp. 271–282, 2004.

[3] K. A. Ford and C. D. Hall, "Singular direction avoidance steering for control-moment gyros," *Journal of Guidance, Control, and Dynamics*, vol. 23, no. 4, pp. 648–656, 2000.

[4] B. Wie, "Singularity escape/avoidance steering logic for control moment gyro systems," *Journal of Guidance, Control, and Dynamics*, vol. 28, no. 5, pp. 948–956, 2005.

[5] F. A. Leve and N. G. Fitz-Coy, "Hybrid steering logic for single-gimbal control moment gyroscopes," *Journal of Guidance Control and Dynamics*, vol. 33, no. 4, pp. 1202–1212, 2010.

[6] F. L. Markley, R. G. Reynolds, F. X. Liu, and K. L. Lebsock, "Maximum torque and momentum envelopes for reaction-wheel arrays," *Journal of Guidance Control and Dynamics*, vol. 33, no. 5, pp. 1606–1614, 2010.

[7] H. Yoon, H. H. Seo, and H.-T. Choi, "Optimal uses of reaction wheels in the pyramid configuration using a new minimum infinity-norm solution," *Aerospace Science and Technology*, vol. 39, pp. 109–119, 2014.

[8] J. D. Boskovic and R. K. Mehra, "Stable multiple model adaptive flight control for accommodation of a large class of control effector failures," in *Proc. Amer. Control Conf.*, San Diego, CA, Jun. 1999, pp. 1920–1924.

[9] Q. Shen, D. W. Wang, S. Zhu, and E. K. Poh, "Integral-type sliding mode fault-tolerant control for attitude stabilization of spacecraft," *IEEE Transactions on Control Systems Technology*, vol. 23, no. 3, pp. 1131–1138, May 2015.

[10] ——, "Inertia-free fault-tolerant spacecraft attitude tracking using control allocation," *Automatica*, vol. 62, pp. 114–121, Dec. 2015.

[11] J. D. Boskovic, S. Li, and R. K. Mehra, "Robust tracking control design for spacecraft under control input saturation," *Journal of Guidance, Control, and Dynamics*, vol. 27, no. 4, pp. 627–633, Jan.-Feb. 2004.

[12] Q. Shen, D. W. Wang, S. Zhu, and E. K. Poh, "Finite-time fault-tolerant attitude stablization for spacecraft with actuator saturation," *IEEE Transactions on Aerospace and Electronic Systems*, vol. 51, no. 3, pp. 2390–2405, Jul. 2015.

[13] B. Wie, *Space Vehicle Dynamics and Control*. AIAA, Reston, VA: AIAA Education Series, 2008.